

Articles

¹⁸³W NMR Study of Peroxotungstates Involved in the Disproportionation of Hydrogen Peroxide into Singlet Oxygen (¹O₂, ¹Δ_g) Catalyzed by Sodium Tungstate in Neutral and Alkaline Water

V. Nardello,[†] J. Marko,[†] G. Vermeersch,[‡] and J. M. Aubry^{*,†}

Equipe de Recherches "Oxydation et Formulation", URA CNRS 351, Cité Scientifique, ENSCL, BP 108, F-59652 Villeneuve d'Ascq Cedex, France, and Laboratoire d'Application RMN, Laboratoire de Physique, URA CNRS 351 Faculté de Pharmacie, BP 83, F-59006 Lille Cedex, France

Received December 29, 1997

The disproportionation of aqueous hydrogen peroxide catalyzed by sodium tungstate has been investigated with regard to the multiplicity of the oxygen molecules released. Trapping experiments and detection of the IR luminescence of ¹O₂ have shown that the yield of ¹O₂ is virtually quantitative. The mono-, di-, and tetraperoxotungstate intermediates W(O₂)_nO_{4-n}²⁻ (n = 1, 2, 4) have been characterized by UV and ¹⁸³W NMR spectroscopies. The diperoxo species is proposed as the precursor of ¹O₂.

Introduction

In 1985, Aubry reported that about thirty inorganic oxides, hydroxides or oxo-anions induce the decomposition of hydrogen peroxide into excited singlet oxygen (¹O₂, ¹Δ_g) in aqueous alkaline medium.¹ Among these new chemical sources of ¹O₂, the system hydrogen peroxide/sodium molybdate appeared particularly attractive on account of its efficiency to generate this excited species in homogeneous phase at room temperature.^{2,3} Since then, much work has been devoted to this system and both the mechanism of the reaction⁴ and its ability to oxidize various organic substrates, in water^{5,6} or in microemulsions,⁷ have been investigated in details. On the other hand, the very similar system hydrogen peroxide/sodium tungstate has been much less studied in terms of singlet oxygen generation^{1,8} whereas it is a well-known epoxidation agent in moderately acidic medium.^{9–11}

Niu and Foote⁸ have recently confirmed the generation of ¹O₂ from the system H₂O₂/WO₄²⁻ by both chemical trapping and detection of the IR luminescence of the excited species. Their study was based on the thermal decomposition of the sodium tetraperoxotungstate, Na₂W(O₂)₄·4H₂O, which was

found to release ¹O₂ at 40 °C in water with a yield of 80%. Nevertheless, the authors specified that this value could be underestimated on account of H₂O₂ decomposition by side reactions. Moreover, as shown recently by Nardello et al.⁴ for the system H₂O₂/MoO₄²⁻, the mono-, di-, tri-, and tetraperoxomolybdates formed in water are in equilibrium and it is likely that a similar behavior also takes place with peroxotungstates. Thus, ¹O₂ detected by warming of a tetraperoxotungstate solution, Na₂W(O₂)₄·4H₂O might be generated by the decomposition of another peroxotungstate.

The aim of the present work was to reinvestigate and to study further the disproportionation of hydrogen peroxide by tungstate ions in neutral and alkaline media. The yield of ¹O₂ formation was reconsidered, the peroxotungstate intermediates were characterized by UV and ¹⁸³W NMR spectroscopies and the precursor of ¹O₂ was identified.

Experimental Section

(1) Reagents. Sodium tungstate dihydrate (99%) was from Aldrich Chemie. Hydrogen peroxide (50% Rectapur) was from Prolabo, Paris. Deuterium oxide (99.8% D) was from CEA (Commissariat à l'Énergie Atomique, Saclay, France). Sodium tetraperoxotungstate Na₂W(O₂)₄·4H₂O,¹² potassium tetraperoxoditungstate K₂[W₂O₃(O₂)₄]·4H₂O,¹³ and tetrapotassium rubrene-2,3,8,9-tetracarboxylate (RTC)¹⁴ were prepared according to known procedures.

(2) Instrumentation. UV/Visible Spectrophotometry. Data were obtained with a Milton Roy Spectronic 3000 spectrophotometer equipped with a diode array photodetector. Full-wavelength scanning measurements can be obtained almost instantaneously, and the detection wavelengths are more reliable than with a scanning spectrophotometer.

¹⁸³W NMR Spectroscopy. The natural abundance ¹⁸³W NMR spectra were recorded on a Bruker AC 300P FT-spectrometer with a 10-mm VSP 300 broad-band probehead. The spectrometer was

[†] Equipe de Recherches "Oxydation et Formulation."

[‡] Laboratoire d'Application RMN.

- (1) Aubry, J. M. *J. Am. Chem. Soc.* **1985**, *107*, 5844–5849.
- (2) Aubry, J. M.; Cazin, B. *Inorg. Chem.* **1988**, *27*, 2013–2014.
- (3) Böhme, K.; Brauer, H.-D. *Inorg. Chem.* **1992**, *31*, 3468–3471.
- (4) Nardello, V.; Marko, J.; Vermeersch, G.; Aubry, J. M. *Inorg. Chem.* **1995**, *34*, 4950–4957.
- (5) Nardello, V.; Bouttemy, S.; Aubry, J. M. *J. Mol. Catal. A: Chem.* **1997**, *117*, 439–447.
- (6) Aubry, J. M.; Cazin, B.; Duprat, F. *J. Org. Chem.* **1989**, *54*, 726–728.
- (7) Aubry, J. M.; Bouttemy, S. *J. Am. Chem. Soc.* **1997**, *119*, 5286–5294.
- (8) Niu, Q. J.; Foote, C. S. *Inorg. Chem.* **1992**, *31*, 3472–3476.
- (9) Fort, Y.; Olzewski-Ortar, A.; Caubere, P. *Tetrahedron* **1992**, *48*, 5099–5110.
- (10) Jorgensen, K. A. *Chem. Rev.* **1989**, *89*, 431.
- (11) Payne, G. B.; Williams, P. H. *J. Org. Chem.* **1959**, *24*, 54–55.

(12) Jahr, K. F.; Lothar, E. *Ber. Dtsch. Chem. Ges.* **1938**, *71*, 894–903.

(13) Stomberg, R. *Acta Chem. Scand.* **1968**, *22*, 1076–1090.

(14) Aubry, J. M.; Rigaudy, J.; Cuong, N. K. *Photochem. Photobiol.* **1981**, *33*, 149–153.

operating at 12.50 MHz and the probe temperature was regulated at 278 ± 1 K. All chemical shifts were referenced to an external $\text{Na}_2\text{WO}_4 \cdot 2\text{H}_2\text{O}$ alkaline solution (2 mol L^{-1}) in D_2O ($\text{pD} = 12$). Typical data acquisition parameters were as follows: pulse duration $20 \mu\text{s}$ (55° flip angle), relaxation delay 0.5 s, sweep width 20833 Hz, time domain 8 K, resolution 1.3 Hz per point. Each sample contained 20% (v/v) D_2O for field frequency locking. 2000 scans were generally sufficient (about 20 min) to obtain an acceptable signal-to-noise ratio. A line-broadening factor (2–5 Hz) was applied before FT.

Singlet Molecular Oxygen Monomer Emission (1270 nm). Infrared emission of $^1\text{O}_2$ was measured with a liquid nitrogen cooled germanium photodiode detector (Model EO-817L, North Coast Scientific Co., Santa Rosa, CA) sensitive in the spectral region from 800 to 1800 nm with a detector of 0.25 cm^2 and a sapphire window. The Ge diode signal was processed with a Lock-in amplifier (model 5205 EG&G, Brookdeal Electronics Princeton Applied Research). An oscilloscope (model 1222A, Hewlett-Packard Co.) was simultaneously used with the amplifier, the chopper and the germanium photodiode detector. The optical chopper (model OC 400, Photon Technology Int.) was used with a frequency of 30 s^{-1} . Measurements were carried out in a cell with mirrored walls ($35 \text{ mm} \times 6 \text{ mm} \times 55 \text{ mm}$).

High-Performance Liquid Chromatography (HPLC). Analyses were carried out with a reverse-phase column (Spherisorb RP 18-50DS) using a Gilson model 303 pump. RTC and RTCO_2 were detected with a $\text{H}_2\text{O}/\text{C}_2\text{H}_5\text{OH}/\text{H}_3\text{PO}_4 = 45:55:0.2$ (v/v) mixture as the eluent and an UV detection at 260 nm with an Holochem H/MD Gilson detector.

(3) Determination of $^1\text{O}_2$ Yield by Chemical Trapping. An aqueous solution in D_2O (5 mL) containing WO_4^{2-} ($10^{-2} \text{ mol L}^{-1}$), EDTA ($2 \times 10^{-4} \text{ mol L}^{-1}$), HCO_3^- ($2 \times 10^{-2} \text{ mol L}^{-1}$), CO_3^{2-} ($2 \times 10^{-2} \text{ mol L}^{-1}$), and H_2O_2 ($10^{-1} \text{ mol L}^{-1}$) was prepared at 0°C . $100 \mu\text{L}$ of this solution was introduced into a tube containing $100 \mu\text{L}$ of RTC ($2 \times 10^{-2} \text{ mol L}^{-1}$) in D_2O . The resulting solution was immersed in a thermostated bath at 25°C and monitored by HPLC for 1 h. Simultaneously, 2.5 mL of the first solution at 0°C were added to 5 mL of H_2SO_4 1/20 at 25°C , and H_2O_2 was titrated with KMnO_4 ($10^{-2} \text{ mol L}^{-1}$).

(4) Determination of the Rates of $^1\text{O}_2$ Formation as a Function of pH. An aqueous (H_2O) buffered solution containing WO_4^{2-} ($10^{-3} \text{ mol L}^{-1}$), RTC ($10^{-4} \text{ mol L}^{-1}$), and EDTA ($10^{-4} \text{ mol L}^{-1}$) was introduced in a spectroscopic cell at 25°C . At time zero, $5 \times 10^{-2} \text{ mol L}^{-1}$ H_2O_2 was added. The evolution of the reaction medium was monitored directly in the cell by UV/visible spectroscopy at 540 nm.

Results

(1) Quantification of the Singlet Oxygen Yield. The yield of $^1\text{O}_2$ formation was measured by chemical trapping with tetrapotassium rubrene-2,3,8,9-tetracarboxylate (RTC) which gives as a sole product the specific endoperoxide RTCO_2 .^{14,15} The excited species was generated from a solution containing initially WO_4^{2-} ($5 \times 10^{-3} \text{ mol L}^{-1}$) and H_2O_2 ($5 \times 10^{-2} \text{ mol L}^{-1}$). The concentration of the trap ($10^{-2} \text{ mol L}^{-1}$) was chosen so that more than 99% of the $^1\text{O}_2$ formed reacts with it instead of being deactivated by water. The formation of RTCO_2 and the loss of RTC were both monitored by HPLC and the initial and final concentrations of H_2O_2 were determined by titration with potassium permanganate. Under such conditions, the yield of $^1\text{O}_2$ formation, $Y(^1\text{O}_2)$ (eq 5), was assessed to $95 \pm 5\%$. This value was confirmed by detection of the specific IR luminescence of $^1\text{O}_2$ at 1270 nm. The intensity I_p emitted by an aqueous solution (H_2O) containing initially WO_4^{2-} ($10^{-1} \text{ mol L}^{-1}$) and H_2O_2 ($6 \times 10^{-1} \text{ mol L}^{-1}$) was measured as a function of time until complete disproportionation was achieved. The resulting curve was compared with that obtained for the system $\text{H}_2\text{O}_2/\text{MoO}_4^{2-}$ under the same conditions (Figure 1). This latter system is known to generate $^1\text{O}_2$ quantitatively^{2,3} and hence,

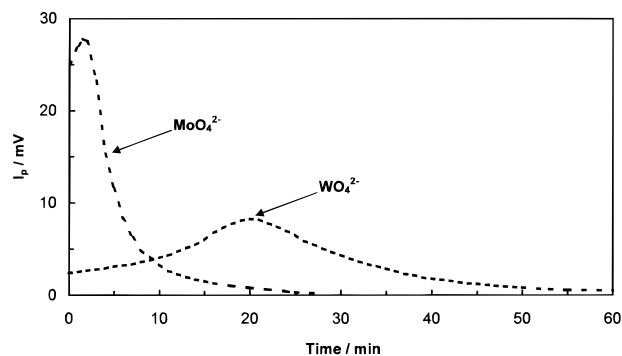


Figure 1. Intensity of the $^1\text{O}_2$ phosphorescence, I_p , emitted at 1270 nm by the systems $\text{H}_2\text{O}_2/\text{MO}_4^{2-}$ where $\text{M} = \text{Mo}, \text{W}$ ($[\text{MO}_4^{2-}] = 10^{-1} \text{ mol L}^{-1}$, $[\text{H}_2\text{O}_2] = 6 \times 10^{-1} \text{ mol L}^{-1}$, $T = 25^\circ\text{C}$, $\text{pH} \geq 10$).

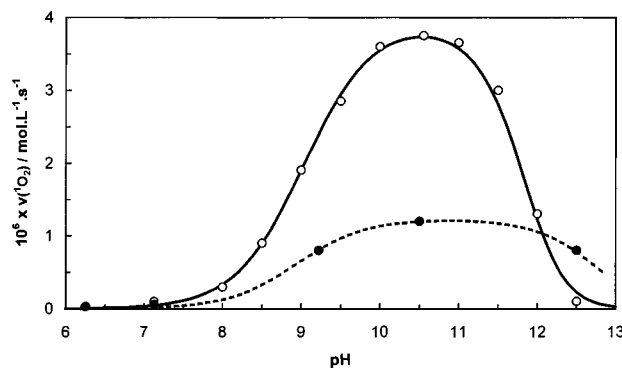


Figure 2. Rates of $^1\text{O}_2$ formation as a function of the pH value for the systems $\text{H}_2\text{O}_2/\text{MO}_4^{2-}$ measured by chemical trapping with RTC ($\text{M} = \text{Mo}$ (○) and W (●), $[\text{MO}_4^{2-}] = 10^{-3} \text{ mol L}^{-1}$, $[\text{H}_2\text{O}_2] = 5 \times 10^{-2} \text{ mol L}^{-1}$, $T = 25^\circ\text{C}$).

by comparing the area below the bell-shaped curves, we found that the yield of $^1\text{O}_2$ formation by the system $\text{H}_2\text{O}_2/\text{WO}_4^{2-}$ is equal to $97 \pm 3\%$.

(2) pH Effect. The rate of $^1\text{O}_2$ formation, $\nu(^1\text{O}_2)$, was measured at different pH values by chemical trapping from solutions containing initially RTC ($10^{-4} \text{ mol L}^{-1}$), WO_4^{2-} ($10^{-3} \text{ mol L}^{-1}$), and H_2O_2 ($5 \times 10^{-1} \text{ mol L}^{-1}$). The trap oxidation was monitored by UV/visible spectroscopy at 540 nm. The evolution of $\nu(^1\text{O}_2)$ according to the pH value is represented in Figure 2. To facilitate the comparison, the curve obtained for the system $\text{H}_2\text{O}_2/\text{MoO}_4^{2-}$ under identical experimental conditions has also been reported.²

As for the system $\text{H}_2\text{O}_2/\text{MoO}_4^{2-}$, the generation of $^1\text{O}_2$ from the system $\text{H}_2\text{O}_2/\text{WO}_4^{2-}$ exhibits a pH-dependence with a maximum around pH 10.5. Nevertheless, at this maximum, the formation of $^1\text{O}_2$ from $\text{H}_2\text{O}_2/\text{WO}_4^{2-}$ occurred about 3.5 times slower than from $\text{H}_2\text{O}_2/\text{MoO}_4^{2-}$.

(3) Identification of the Peroxotungstate Intermediates.

(3.1) Influence of the Hydrogen Peroxide Concentration.

^{183}W NMR Spectroscopy. Concentrated (1 mol L^{-1}) solutions of sodium tungstate were used in order to obtain ^{183}W NMR data on a relatively short time scale (≈ 20 min). The temperature was kept at 278 K to minimize changes during the recording of the spectra and to avoid precipitation of the peroxotungstates which are much less water-soluble than the corresponding peroxomolybdates. The spectra of two well-defined crystallized peroxotungstates were first recorded: (i) sodium tetraperoxotungstate $\text{Na}_2\text{W}(\text{O}_2)_4 \cdot 4\text{H}_2\text{O}$ (1 mol L^{-1}) dissolved into 5.6 mol L^{-1} of H_2O_2 ($\text{pH} = 6.5$) (spectrum a) and (ii) potassium tetraperoxoditungstate $\text{K}_2[\text{W}_2\text{O}_3(\text{O}_2)_4] \cdot 4\text{H}_2\text{O}$ ($5 \times 10^{-2} \text{ mol L}^{-1}$) dissolved in pure water ($\text{pH} = 5.5$) (spectrum f). Then, we investigated molar solutions of sodium tungstate with increasing

(15) Nardello, V.; Brault, D.; Chavalle, P.; Aubry, J. M. *J. Photochem. Photobiol. B* **1997**, *39*, 146–155.

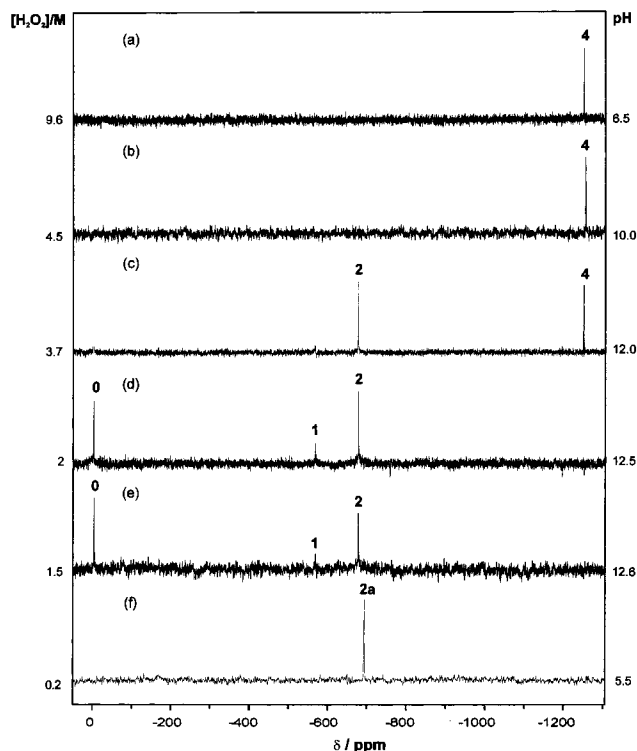


Figure 3. ^{183}W NMR spectra (b–e) of peroxotungstates formed as a function of the initial total concentration of H_2O_2 ($T = 278\text{ K}$, natural pH, $[\text{Na}_2\text{WO}_4] = 1\text{ mol L}^{-1}$). (a) Tetraperoxotungstate $\text{Na}_2\text{W}(\text{O}_2)_4 \cdot 4\text{H}_2\text{O}$ (1 mol L^{-1}) dissolved in aqueous H_2O_2 (5.6 mol L^{-1}); (f) tetraperoxoditungstate $\text{K}_2[\text{W}_2\text{O}_3(\text{O}_2)_4] \cdot 4\text{H}_2\text{O}$ ($5 \times 10^{-2}\text{ mol L}^{-1}$) dissolved in pure water.

concentrations of H_2O_2 at natural pH (>10.0) (Figure 3). The NMR spectra exhibit four narrow peaks, **0** ($\delta = 0\text{ ppm}$), **1** ($\delta = -567\text{ ppm}$), **2** ($\delta = -676\text{ ppm}$), and **4** ($\delta = -1247\text{ ppm}$), which successively appear at upfield shifts as the H_2O_2 concentration increases.

UV Spectrophotometry. To facilitate the comparison with the ^{183}W NMR results, the UV absorption spectra were recorded for solutions obtained under similar experimental conditions ($[\text{WO}_4^{2-}] = 1\text{ mol L}^{-1}$, various $[\text{H}_2\text{O}_2]$, natural pH, $T = 278\text{ K}$). The molar aqueous solution of sodium tungstate was initially colorless. Then, a yellow coloration progressively appeared when H_2O_2 was added. The absorbance was measured at 325 nm after dilution in methanol (1/400) in order to avoid hydrolysis of the peroxotungstates and to minimize the absorption due to H_2O_2 . At this wavelength, the absorption is essentially due to the tetraperoxotungstate, $\text{W}(\text{O}_2)_4^{2-}$, the most peroxidized intermediate ($\epsilon_{325\text{ nm}} = 430\text{ L mol}^{-1}\text{ cm}^{-1}$). The evolution of the absorbance at 325 nm as a function of H_2O_2 concentration is reported in Figure 4.

Figure 4 shows that the formation of the tetraperoxotungstate $\text{W}(\text{O}_2)_4^{2-}$ occurs at lower concentrations of H_2O_2 than those required for the formation of the tetraperoxomolybdate $\text{Mo}(\text{O}_2)_4^{2-}$. In the first case, the binding of H_2O_2 on W nucleus is almost quantitative whereas the peroxidation of molybdate is complete only with a large excess of H_2O_2 .⁴ Under such conditions, the amount of free H_2O_2 , i.e., not bound to the tungsten atom, cannot be assessed and thus the equilibrium constants cannot be inferred. Therefore, the equilibrium established between the tetraperoxotungstate $\text{W}(\text{O}_2)_4^{2-}$ and a less peroxidized intermediate was investigated with more dilute aqueous solutions of sodium tungstate ($2 \times 10^{-3}\text{ mol L}^{-1}$) at pH = 10.0. The

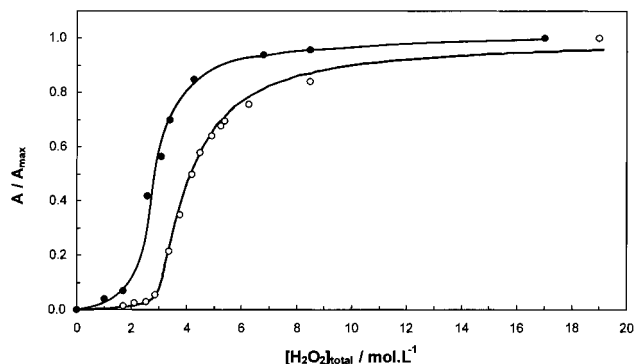


Figure 4. Influence of the concentration of H_2O_2 on the absorbance of a molar sodium tungstate solution (\bullet) at 325 nm after dilution in CH_3OH (1/400) ($[\text{WO}_4^{2-}] = 1\text{ mol L}^{-1}$, natural pH, $T = 278\text{ K}$). Comparison with sodium molybdate (\circ).⁴

absorbance was measured in the decreasing part of the spectrum at 350 nm .¹⁶

(3.2) Influence of Acidity. ^{183}W NMR Spectroscopy. When $[\text{H}_2\text{O}_2]/[\text{WO}_4^{2-}] = 8$, a single peak **4** ($\delta = -1247\text{ ppm}$) was observed at natural pH (7.15). When increasing amounts of concentrated hydrochloric acid were added, peak **4** progressively disappeared whereas peak **2a** ($\delta = -699\text{ ppm}$) increased. Peak **4** exhibits the same chemical shift as that obtained for the tetraperoxoditungstate (spectrum f). On the other hand, when $[\text{H}_2\text{O}_2]/[\text{WO}_4^{2-}] = 3.7$, the spectrum obtained at natural pH (12.0) exhibited peaks **2** ($\delta = -676\text{ ppm}$) and **4** with nearly equal intensities (Figure 3c). In the same manner, as the pH was lowered by addition of concentrated HCl, peak **2** was replaced by peak **2a** whereas peak **4** was still present until pH ≈ 5.0 . From pH 5.0 to 0.0, only peak **2a** was observed. A similar behavior was observed when $[\text{H}_2\text{O}_2]/[\text{WO}_4^{2-}] = 2$, except that the spectrum exhibited, at natural pH (12.5), peak **1** ($\delta = -567\text{ ppm}$) in addition to the others.

UV Spectrophotometry. As the tetraperoxotungstate, $\text{W}(\text{O}_2)_4^{2-}$, can be specifically detected by UV spectroscopy, the influence of the pH on the stability of this peroxocomplex could be studied. A solution containing initially WO_4^{2-} ($10^{-2}\text{ mol L}^{-1}$) and H_2O_2 (1 mol L^{-1}) was titrated, on the one hand, with NaOH (5 mol L^{-1}) and, on the other hand, with HCl (1 mol L^{-1}). Under the initial conditions, the natural pH of the solution was equal to 8.5 and the prevalent species was the tetraperoxotungstate. The evolution of the reaction medium, by addition of acid or base, was followed by UV spectroscopy in the decreasing part of the spectrum at 380 nm .¹⁶

Discussion

(1) Singlet Oxygen Yield. One method currently used for the quantification of $^1\text{O}_2$ formed during a process occurring in aqueous solution consists of trapping chemically this excited species with a specific water-soluble trap such as RTC.^{1,2,15} Thus, in the presence of this trap, $^1\text{O}_2$ formed in the reaction medium can either react with it (eq 1) according to the second-order rate constant k_t or be quenched by water (eq 2) according to the pseudo-first-order rate constant k_d :¹⁷



(16) Supporting Information.

(17) Wilkinson, F.; Helman, W. P.; Ross, A. B. *J. Phys. Chem. Ref. Data* **1995**, *24*, 671.



Under steady-state conditions ($d[{}^1\text{O}_2]/dt = 0$) and after integration between zero time and t , we obtain the following expression for the cumulative amount of ${}^1\text{O}_2$:¹⁷

$$[{}^1\text{O}_2]_t = [\text{RTC}]_0 - [\text{RTC}]_t + \frac{k_d}{k_r} \ln \frac{[\text{RTC}]_0}{[\text{RTC}]_t} \quad (3)$$

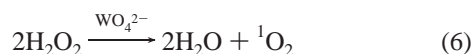
Under our experimental conditions, the quenching of ${}^1\text{O}_2$ by water (eq 2) is negligible compared to the trapping reaction (eq 1) and hence, eq 3 simplifies into

$$[{}^1\text{O}_2]_t = [\text{RTC}]_0 - [\text{RTC}]_t \quad (4)$$

The yield of ${}^1\text{O}_2$ formation, $Y({}^1\text{O}_2)$, is defined as the ratio of the cumulative amount of ${}^1\text{O}_2$ over the total amount of oxygen generated by the catalytic disproportionation of H_2O_2 . It can easily be determined from the loss of RTC and H_2O_2 according to the following relation:

$$Y({}^1\text{O}_2) = \frac{[{}^1\text{O}_2]_t}{[\text{O}_2]_t} = \frac{[\text{RTC}]_0 - [\text{RTC}]_t}{0.5([\text{H}_2\text{O}_2]_0 - [\text{H}_2\text{O}_2]_t)} \quad (5)$$

This led to a value of $95 \pm 5\%$ for the yield of ${}^1\text{O}_2$ generation from the system $\text{H}_2\text{O}_2/\text{WO}_4^{2-}$ according to eq 6:



A second method used to determine $Y({}^1\text{O}_2)$ consists of the detection of the IR luminescence of ${}^1\text{O}_2$ at 1270 nm accompanying the radiative deactivation of ${}^1\text{O}_2$ according to a rate constant k_p (eq 7):³



Although this pathway is completely negligible compared with the deactivation of ${}^1\text{O}_2$ by the solvent (eq 2), it is very useful to monitor the stationary concentration of ${}^1\text{O}_2$.³ The intensity I_p of the phosphorescence emission is given by $I_p = ck_p[{}^1\text{O}_2]_s$, where c is a constant of the spectrometer and $[{}^1\text{O}_2]_s$ represents the stationary concentration of ${}^1\text{O}_2$. In an aqueous solution free of trap, $[{}^1\text{O}_2]_s$ is set from the dynamic equilibrium between the two major processes (eq 2 and 6). Thus, $[{}^1\text{O}_2]_s = \nu({}^1\text{O}_2)/k_d$ where $\nu({}^1\text{O}_2)$ is the rate of ${}^1\text{O}_2$ generation from reaction (6). The cumulative amount of ${}^1\text{O}_2$ generated in the reaction medium between zero and infinite time may then be expressed as

$$[{}^1\text{O}_2]_\infty = \int_0^\infty \nu({}^1\text{O}_2) dt = k_d \int_0^\infty [{}^1\text{O}_2]_s dt = \frac{k_d}{ck_p} \int_0^\infty I_p dt \quad (8)$$

Therefore, the area below the curve representing the evolution of the intensity I_p versus time (Figure 1) is directly proportional to the cumulative amount of ${}^1\text{O}_2$ generated. By taking as a reference the system $\text{H}_2\text{O}_2/\text{MoO}_4^{2-}$ which releases ${}^1\text{O}_2$ quantitatively,^{2,3} $Y({}^1\text{O}_2)$ was estimated to $97 \pm 3\%$. This value is in good agreement with the result obtained by chemical trapping and confirms that the system $\text{H}_2\text{O}_2/\text{WO}_4^{2-}$ generates ${}^1\text{O}_2$ quantitatively, like the system $\text{H}_2\text{O}_2/\text{MoO}_4^{2-}$.^{2,3}

On the other hand, the lower curve in Figure 1 shows that, under the initial conditions ($[\text{WO}_4^{2-}] = 0.1 \text{ mol L}^{-1}$, $[\text{H}_2\text{O}_2] = 0.6 \text{ mol L}^{-1}$) for which an excess of H_2O_2 was introduced,

Table 1. ¹⁸³W NMR Data, Experimental Conditions, and Assignments for the Different Peaks Observed at 278 K with the $\text{WO}_4^{2-}/\text{H}_2\text{O}_2/\text{H}^+$ System ($[\text{WO}_4^{2-}] = 1 \text{ mol L}^{-1}$)

peak no.	δ (ppm)	$[\text{H}_2\text{O}_2]/[\text{WO}_4^{2-}]$	pH range	assignments
0	0	0–2	7–14	WO_4^{2-}
1	–567	<2	10–14	$\text{WO}_3(\text{O}_2)^{2-}$
2	–676	<4	9–14	$\text{WO}_2(\text{O}_2)_2^{2-}$
2a	–699	>1	<9	$\text{W}_2\text{O}_3(\text{O}_2)_4^{2-}$
4	–1247	>3	4–14	$\text{W}(\text{O}_2)_4^{2-}$

the major peroxotungstate formed, i.e., the tetraperoxotungstate, is not the main precursor of ${}^1\text{O}_2$ since the luminescence intensity increased at first as the disproportionation of H_2O_2 proceeded and then decreased. In addition, comparison of the tungstate and the molybdate curves indicates that the maximum rate of ${}^1\text{O}_2$ formation is about 3.5 times slower when H_2O_2 is decomposed by tungstate instead of molybdate ions.

(2) Identification of the Peroxotungstates by ¹⁸³W NMR.

(2.1) Crystallized Peroxotungstates. The tungsten peroxo-complexes are very similar to the molybdenum complexes.^{18,19} Some of them have been isolated as monocrystals and thoroughly structurally characterized by X-ray diffraction, in particular, the potassium tetraperoxotungstate $\text{K}_2[\text{W}(\text{O}_2)_4]$ and the potassium tetraperoxoditungstate $\text{K}_2[\text{W}_2\text{O}_3(\text{O}_2)_4] \cdot 4\text{H}_2\text{O}$.^{20,21} We recorded the ¹⁸³W NMR spectra of these two species by dissolving the crystallized compounds under conditions of pH and H_2O_2 concentration ensuring their stability. The resulting data are reported in Table 1 and Figure 3. The comparison of the spectra recorded for the system $\text{H}_2\text{O}_2/\text{WO}_4^{2-}/\text{H}^+$ allowed us to unambiguously assign some of these peaks.

The NMR spectrum of an aqueous solution ($5 \times 10^{-2} \text{ mol L}^{-1}$) of an authentic sample of $\text{K}_2[\text{W}_2\text{O}_3(\text{O}_2)_4] \cdot 4\text{H}_2\text{O}$ at natural pH (5.5) mainly shows the peak **2a** ($\delta = -699 \text{ ppm}$) which was assigned to the tetraperoxoditungstate $\text{W}_2\text{O}_3(\text{O}_2)_4^{2-}$, in agreement with Campbell et al.²² The peak **4** ($\delta = -1247 \text{ ppm}$) could be assigned to the tetraperoxotungstate, $\text{W}(\text{O}_2)_4^{2-}$, the most peroxidized species.²³ Actually, it is the only peak observed either when 1 mol L⁻¹ sodium tungstate is dissolved in neutral or alkaline concentrated H_2O_2 (spectrum b) or when 1 mol L⁻¹ of a genuine sample of sodium tetraperoxotungstate $\text{Na}_2\text{W}(\text{O}_2)_4 \cdot 4\text{H}_2\text{O}$ is dissolved into 5.6 mol L⁻¹ H_2O_2 (spectrum a).

(2.2) Peroxotungstates in Solution. When the ¹⁸³W NMR spectra were recorded at natural pH with various H_2O_2 concentrations (Figure 3), peaks **1**, **2**, and **4** could be detected besides the peak **0** ($\delta = 0 \text{ ppm}$) which corresponds to the tungstate ion WO_4^{2-} (see Table 1). The assignments of peaks **1** ($\delta = -567 \text{ ppm}$) and **2** ($\delta = -676 \text{ ppm}$) are less straightforward than those of peaks **2a** and **4**. The recording of the ¹⁸³W NMR spectra of a solution containing initially WO_4^{2-} (1 mol L⁻¹) and H_2O_2 (4.5 mol L⁻¹) shows that peak **4**, then peak **2** and peak **1** and finally, peak **0** successively appear as H_2O_2 is decomposed. In addition, we can notice that peak **2** is always more intense than peak **1**. By taking into account these observations and the findings obtained by UV spectroscopy which demonstrate the involvement of an equilibrium between the tetraperoxotungstate $\text{W}(\text{O}_2)_4^{2-}$ and the diperoxotungstate

(18) Dickman, H. M.; Pope, M. T. *Chem. Rev.* **1994**, *94*, 574–584.

(19) Connor, J. A.; Ebsworth, E. A. V. *Adv. Inorg. Chem. Radiochem.* **1964**, *6*, 313–323.

(20) Stomberg, R. J. *Less-Common Met.* **1988**, *143*, 363–371.

(21) Einstein, F. W. B.; Penfold, B. R. *Acta Crystallogr.* **1963**, *16* (Supplement), A35.

(22) Campbell, N. J.; Dengel, A. C.; Edwards, C. J.; Griffith, W. P. *J. Chem. Soc., Dalton Trans.* **1989**, 1203–1208.

(23) Nakajimi, H.; Kudo, T.; Mizuno, N. *Chem. Lett.* **1997**, 693–694.

$\text{WO}_2(\text{O}_2)_2^{2-}$ (see below), peak **2** is assigned to this latter species. On the other hand, we assume that peak **1** probably corresponds to the monoperoxotungstate $\text{WO}_3(\text{O}_2)^{2-}$. Actually, Nardello et al.⁴ and Nakajima et al.²³ showed that the chemical shift of the peroxomolybdates and the peroxotungstates increases with the number of peroxo groups. Hence, the peak **1**, which appears at -567 ppm, at low concentrations of H_2O_2 , is assigned to a monoperoxo species. The different NMR spectra obtained and their interpretation do not provide any evidence with regard to the formation of a possible triperoxotungstate $\text{WO}(\text{O}_2)_3^{2-}$, analogous to the complex $\text{MoO}(\text{O}_2)_3^{2-}$ detected with the system $\text{H}_2\text{O}_2/\text{MoO}_4^{2-}$ and whose the chemical shift should lie between -700 and -1247 ppm. This result could be an explanation of the well-known greater stability of the system $\text{H}_2\text{O}_2/\text{WO}_4^{2-}$ in alkaline medium since it has been shown that the triperoxo-metalate is the main intermediate in the disproportionation of H_2O_2 catalyzed by MoO_4^{2-} .⁴ However, the formation of the triperoxotungstate cannot be completely ruled out and it is possible that this species is formed in such a low concentration that it could not be detected by ^{183}W NMR.

On the other hand, the results obtained when increasing amounts of hydrochloric acid were added to solutions containing initially WO_4^{2-} (1 mol L^{-1}) and H_2O_2 ($2, 3.7, \text{ or } 8 \text{ mol L}^{-1}$) show that, under our conditions and whatever the concentration of H_2O_2 is, the only peroxo compound present in solution from about pH 9 to 0, was the tetraperoxoditungstate $\text{W}_2\text{O}_3(\text{O}_2)_4^{2-}$. Hence, the formation of a triperoxo dimer, similar to that one identified in the case of the system $\text{H}_2\text{O}_2/\text{MoO}_4^{2-}$ in neutral media at high concentrations of H_2O_2 , i.e., $[\text{MoO}(\text{O}_2)_2\text{OOH}]_2^{2-}$,⁴ has not been detected.

Nakajima et al.²³ have recently reported a ^{183}W NMR study of the peroxotungstates formed by reaction of tungsten metal powder with H_2O_2 . They detected four signals at $-697, -621, -392,$ and -300 ppm. The first one, in agreement with our result, was assigned to $\text{W}_2\text{O}_3(\text{O}_2)_4^{2-}$. On the other hand, we did not observe in our ^{183}W NMR study of the system $\text{H}_2\text{O}_2/\text{WO}_4^{2-}$ any peak at $-621, -392,$ or -300 ppm. The authors assigned the peak at -621 ppm either to the diperoxotungstate $\text{WO}_2(\text{O}_2)_2^{2-}$ or to $[\text{WO}(\text{O}_2)_2(\text{OH})]^-$ and/or to the corresponding protonated species, as the chemical shift of this peak is very sensitive toward pH variations. No data concerning the concentrations of the species ($\text{W}, \text{H}_2\text{O}_2, \text{H}^+$) present in solution at the moment of the recording of ^{183}W NMR spectra are available in Nakajima's report. Nevertheless, if we refer to the experimental conditions, we can calculate these concentrations by assuming that tungsten metal is oxidized according to eq 9.



Thus, the spectra recorded by the authors would correspond to a solution containing the following reactants: $[\text{WO}_4^{2-}] = 0.86 \text{ mol L}^{-1}$, $[\text{H}_2\text{O}_2] = 3.85 \text{ mol L}^{-1}$, $[\text{H}^+] = 1.7 \text{ mol L}^{-1}$. Such concentrations provide a strongly acidic medium and the alkaline species $\text{W}(\text{O}_2)_n\text{O}_{4-n}^{2-}$ are readily converted into their mono- and/or diprotonated forms, as confirmed by the stability of this reaction medium after 1 and 24 h. Hence, it is very likely that the peak at -621 ppm would correspond to the monoprotonated diperoxotungstate $[\text{WO}(\text{O}_2)_2(\text{OH})]^-$ whereas the peak at -676 ppm that we have observed would rather correspond to the dianionic diperoxotungstate $\text{WO}_2(\text{O}_2)_2^{2-}$. At last, the peaks at -392 and -300 ppm, which were assigned respectively to a dimer and a monomer species ($\text{O}_2^{2-}/\text{W} = 1$, for both) were not detected under our conditions.

(3) Equilibria Between the Tetraperoxotungstate and Less Peroxidized Complexes. (3.1) Influence of Acidity.

The influence of the acidity on $\text{W}(\text{O}_2)_4^{2-}$ was investigated by UV spectroscopy at 380 nm .¹⁶ Contrary to the NMR experiments for which concentrated solutions were used ($[\text{WO}_4^{2-}] = 1 \text{ mol L}^{-1}$), the UV analysis had to be performed in more dilute media with $[\text{WO}_4^{2-}] = 10^{-2} \text{ mol L}^{-1}$. Under such conditions, we can consider that only monomer species are present in solution. Under such conditions, we can consider that only monomer species are present in solution. The curve obtained indicates that the reaction requires only one equivalent of HCl. Hence, $\text{W}(\text{O}_2)_4^{2-}$ is converted, by addition of acid, into the monoprotinated diperoxotungstate $\text{HWO}_2(\text{O}_2)_2^-$ according to eq 10.



The constant K of this equilibrium is defined by the following relation:

$$K = \frac{[\text{W}(\text{O}_2)_4^{2-}][\text{H}_3\text{O}^+]}{[\text{HWO}_2(\text{O}_2)_2^-][\text{H}_2\text{O}_2]_{\text{free}}^2} \quad (11)$$

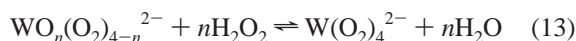
where $[\text{H}_2\text{O}_2]_{\text{free}} = [\text{H}_2\text{O}_2]_{\text{total}} - 4[\text{W}(\text{O}_2)_4^{2-}] - 2[\text{HWO}_2(\text{O}_2)_2^-]$.

A linear relationship between the absorbance at 380 nm of $\text{W}(\text{O}_2)_4^{2-}$ ($\epsilon_{380 \text{ nm}} = 132 \text{ L mol}^{-1} \text{ cm}^{-1}$) and the free H_2O_2 concentration can be established according to eq 12, where $A_{\text{tetra}} = 1.32$ is the higher value of the absorbance of $\text{W}(\text{O}_2)_4^{2-}$ at 380 nm .

$$\log \frac{A}{A_{\text{tetra}} - A} = \log K + \text{pH} + 2 \log [\text{H}_2\text{O}_2]_{\text{free}} \quad (12)$$

When eq 12 is applied to the experimental result, a linear plot is obtained.¹⁶ The calculated slope is 1.00 and the intercept is -6.72 leading to $K = 2 \times 10^{-7}$ for the equilibrium (10).

(3.2) Influence of H_2O_2 Concentration. In a same way, for a constant pH value equal to 10.0, the UV spectroscopy allowed us to determine the number n of H_2O_2 molecules exchanged in the equilibrium involving the tetraperoxocomplex and a less peroxidized intermediate, $\text{WO}_n(\text{O}_2)_{4-n}^{2-}$ ($n = 1, 2, 3$) (eq 13).



The constant K of this equilibrium is defined by the following relation:

$$K = \frac{[\text{W}(\text{O}_2)_4^{2-}]}{[\text{WO}_n(\text{O}_2)_{4-n}^{2-}][\text{H}_2\text{O}_2]_{\text{free}}^n} \quad (14)$$

Under the experimental conditions used ($[\text{WO}_4^{2-}] = 2 \times 10^{-3} \text{ mol L}^{-1}$), we can consider that the concentrations of free and total H_2O_2 are almost equal. Thus, a linear relationship between the absorbance of $\text{W}(\text{O}_2)_4^{2-}$ at 350 nm ($\epsilon_{350 \text{ nm}} = 375 \text{ L mol}^{-1} \text{ cm}^{-1}$) and the concentration of free H_2O_2 can be established according to eq 15, where $A_{\text{tetra}} = 0.75$ is the maximum value of the absorbance of $\text{W}(\text{O}_2)_4^{2-}$ at 350 nm and n represents the number of H_2O_2 molecules exchanged in the equilibrium (13).

$$\log \frac{A}{A_{\text{tetra}} - A} = \log K + n \log [\text{H}_2\text{O}_2]_{\text{free}} \quad (15)$$

When eq 15 is applied to the experimental results, a linear plot is obtained.¹⁶ The calculated slope is 1.92, and the intercept is 1.83 leading to $K = 67.6$. The first value confirms the

participation of two molecules of H₂O₂ in the equilibrium under study whereas for the system H₂O₂/MoO₄²⁻, only one molecule of H₂O₂ was found to be exchanged, in agreement with the involvement of a triperoxomolybdate.⁴ Therefore, this result shows that, in the case of the system H₂O₂/WO₄²⁻, the tetraperoxotungstate is in equilibrium with the diperoxotungstate WO₂(O₂)₂²⁻ according to eq 13 with $n = 2$. In addition, if we compare the equilibrium constants involving respectively the tetraperoxotungstate and the tetraperoxomolybdate and a less peroxidized intermediate, we see that only 0.12 mol L⁻¹ of free H₂O₂ is required to obtain 50% of W(O₂)₄²⁻ whereas 50% of Mo(O₂)₄²⁻ is formed in the presence of 0.71 mol L⁻¹ of free H₂O₂. These values indicate that the tungsten complex is much more stable than its molybdenum homologous, what is confirmed by the curves obtained in concentrated media (see Figure 4). Such a greater stability might result from the structure of these complexes which have both been described as distorted dodecahedra on the basis of a tetrahedral arrangement of the four η²-O₂²⁻ ligands.^{20,24} Nevertheless, in the case of the tungsten nucleus, we can assume that there is less steric hindrance between the four peroxo bridges than in the case of the molybdenum nucleus. The greater stability of W(O₂)₄²⁻ would impede the formation of a triperoxo intermediate. Accordingly, for the system H₂O₂/W(O₂)₄²⁻, the main precursor of singlet oxygen should be the diperoxotungstate WO₂(O₂)₂²⁻, and not the triperoxo complex as for the system H₂O₂/MoO₄²⁻.

(24) Stomberg, R. *Acta Chem. Scand.* **1969**, *23*, 2755–2763.

It is noteworthy that, for this latter system, the diperoxo complex, MoO₂(O₂)₂²⁻, had also been shown to generate ¹O₂ but to a lesser extent.⁴

Conclusion

The system H₂O₂/WO₄²⁻ behaves in many ways very similarly to the system H₂O₂/MoO₄²⁻ since it also generates ¹O₂ quantitatively although the rate of the formation of the excited species is about 3.5 times slower. The study by ¹⁸³W NMR spectroscopy allowed to identify the mono-, di-, and tetraperoxotungstates homologous to the corresponding peroxomolybdates. Therefore, in the case of the system H₂O₂/WO₄²⁻, the main precursor of ¹O₂ should be the diperoxotungstate, WO₂(O₂)₂²⁻, in agreement with a lower rate of H₂O₂ disproportionation. However, the expected oxotriperoxotungstate was not detected since the diperoxotungstate is directly converted into the tetraperoxotungstate because this later complex was shown to be much more stable than the tetraperoxomolybdate.

Acknowledgment. We are grateful to H. Sies and K. Briviba for help with the experiments of the IR luminescence of ¹O₂.

Supporting Information Available: Figures showing the evolution of the absorbance at 350 and 380 nm according to the H₂O₂ concentration and the pH value, respectively, and corresponding linear plots (2 pages). Ordering information is given on any current masthead page.

IC971607S